First principles study of SnS electronic properties using LDA, PBE and HSE06 functionals

R. Ibragimova[1], M. Ganchenkova[1], S. Karazhanov[1,2] and E. S. Marstein[2]

[1]Department of Materials Science, National Research Nuclear University "MEPhI", 31 Kashirskoe sh, 115409 Moscow, Russia

[2]Department for Solar Energy, Institute for Energy Technology, PO Box 40, 2027 Kjeller, Norway

Abstract

In recent years, tin sulfide (SnS) has emerged as a promising alternative to conventional CIGS and CZTC solar cells because of the suitable electronic properties. Despite the rapid development of SnS in solar cells application, the performance of the devices based on is still low. One of the reasons is poorly understood properties of the material. The goal of this work the is a study of electronic structure using theoretical approaches. We studied the electronic properties of SnS using several exchange-correlation functionals such as LDA, PBE, and HSE06. The large variation of bandgap appears in previous theoretical reports as well as in this work. We have supposed that the variation is related to an appeared excessive hydrostatic pressure due to using not sufficiently relaxed lattice parameters. The analysis shows that HSE06 functional has the best match with experimentally obtained valence band spectra from XPS measurements. However, besides underestimation of bandgap, LDA shows the satisfactory agreement with valence band XPS spectrum .

Introduction

Technologies of solar cells are the rapidly growing field recently. Great effort has been made in the developing of new concepts and design of devices, but the major challenge is a correct selection of device materials in order to achieve a high energy conversion and cost efficiency. For this reason, the main attention is given to the development and improvement of new materials for solar cells application. As a result, four generations of solar cells based on different materials and production technologies have been developed already. Thinfilm solar cells are related to the second generation solar cells, that provides low cost of a device due to lower material consumption. Recently developed Cu(In,Ga)Se$_2$ (CIGS) and Cu$_2$(ZnSn)(SSe)$_4$ (CZTS) are the best known thinfilm materials at the moment. These materials have a reported efficiency of about 18 % that is still less than performance of best market solar cells. Moreover, there are number of shortcomings of these thinfilm materials such as a lack of production stability, the expensive composed materials, and toxicity, which prevent increasing an efficiency and producing it on a market scale. Though there is an active research interest, new breakthroughs are still under way, according to the published data.

Recently, tin sulfide has been proposed as one of the promising absorbance materials in thin film technologies due to its suitable properties such as absorption coefficient above 10^4 cm^{-1}, high carrier mobility, p- or n-type of conductivity [1] and the bandgap 1.1-1.4 eV close to optimal value [2]. In distinction from mentioned above materials, tin sulfide possesses such properties as nontoxicity, low cost, and production stability. SnS has a high theoretically predicted efficiency above 20%, but at the moment the experimentally achieved one is only 4.36 % [3] [4]. The reason of low achieved efficiency is unclear, probably, due to poorly understood nature of the material. There are a lot of studies carried out in that respect, but still underexplored properties such as the generation-recombination processes of charge carriers, defects, and impurities behavior, doping parameters, the interface effects, and the undeveloped fabrication methods hinder to develop an improved device [2].

The combination of theoretical modelling and experiments is an efficient approach to achieve comprehensive understanding of the material features and decreasing the research expenses at the same time. One of the most advanced methods of modeling is Density Functional Theory (DFT) based method, which allows describing electronic and optical properties. Even though, DFT is a powerful tool in computational physics, the method has some limitations and restrictions. In fact, conventional DFT has a problem of the bandgap underestimation that prevents producing an accurate prediction of materials properties. In order to overcome the bandgap underestimation problem some other approaches has been produced, such as hybrid functional based method [14] and many-body perturbation method GW [15]. SnS has been the

subject of theoretical studies by using all of the mentioned. For example, the electronic structures have been carried out previously in the literature [5-11] using Local Density Approximation (LDA) [12], General Gradient Approximation (GGA) [13], hybrid functionals [14] and many-body perturbation theory GW [15]. Analysis of the literature data shows that calculated bandgap values have a large variation from 0.26 to 1.26 eV, whereas experimentally measured values vary in the interval of 1.1-1.4 eV [2]. Moreover, the variation of bandgap appears in values calculated within the same exchange-correlation functional, in spite of the fact that results within the same functional should coincide in the range of error. For instance, according to the reported data [7,10,27], obtained based on LDA bandgap varies from 0.26 eV to 0.72 eV from paper to paper. Having in mind the final goal of the study and importance of defect physics for any of opto-electronic devices, we should be able to describe defect properties with a certain level of accuracy. In this respect, we must be confident about the accuracy of the basic electronic properties calculation and respectively make an appropriate choice ща exchange-correlation functional with understanding of any source of errors. That is why, this paper is dedicated to the systematic study of the applicability of LDA, PBE and hybrid functional to electronic properties calculations in order to choose the best one and clarify the reason of bandgap variation.

2. Computational details

This work is divided in two steps: the first is to check the most energetically favored polymorph of SnS and the second one is to calculate the electronic properties of selected polymorph using several exchange-correlation functionals. The calculations have been performed using The Vienna Ab-initio Simulation Package (VASP) [16]. In the first step, we considered several polymorphic modifications of SnS of different space groups: CmCm, C2mb, Fm-3m, Pnma, in order to theoretically verify the most energetically favored one. For full structure optimization of all polymorphic modifications has been used the generalized gradient approximation (GGA) with Perdew-Burke-Ernzerhof (PBE) [13] exchange-correlation functional together with the projector-augmented waves (PAW) [17] method. The optimal plane wave cutoff energy, k-points mesh has been chosen based on performed total energy convergence test.

Furthermore, the structural optimization was performed for the chosen polymorph with Pnma space group containing 8 atoms in unit cell. As the second step, several exchange-correlation functionals and methods has been used for the electronic properties calculations. We have used LDA [12] and PBE [13] exchange-correlation functionals in the frame of conventional DFT. The optimal parameters for each of the functional were chosen as 2x3x3 k-point sampling and 600 eV cutoff energy, according to the performed total energy convergence test. Total energy dependence on the set of k-points is shown in Fig.1.
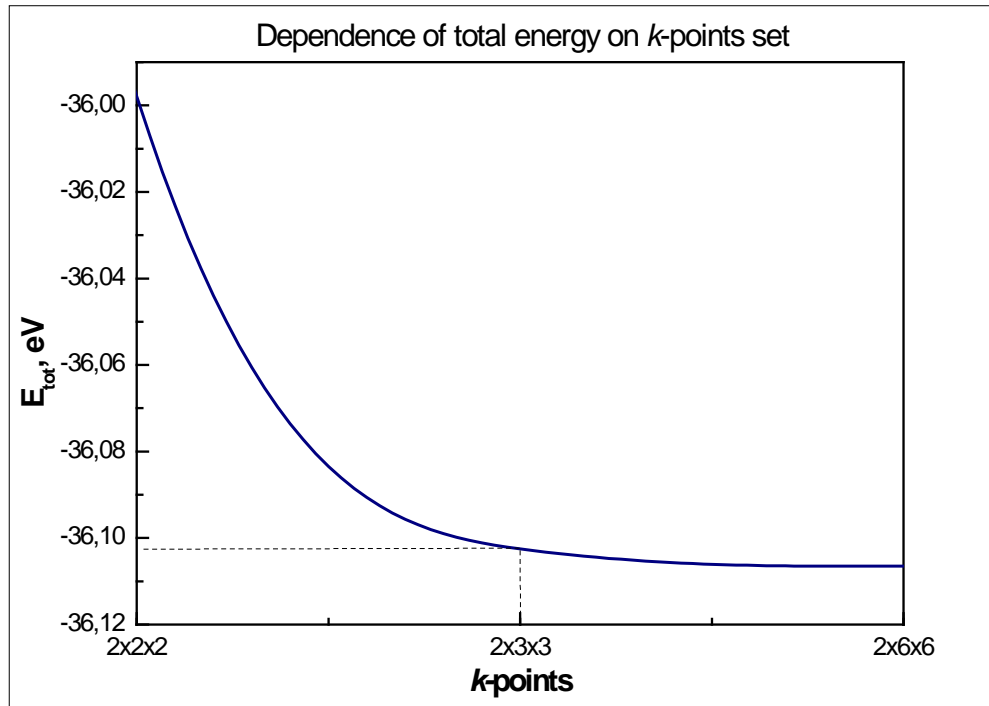
Fig. 1 - Dependence of total energy on k-points set

Knowing that, conventional DFT usually underestimates a bandgap of semiconductors [18], we have also used hybrid functional in a form proposed by Heyd-Scuseria-Ernzerhof (HSE06) [19], which includes a fraction of exact exchange (Hartree-Fock) and correlation terms. In the hybrid functional, the following range separation and mixing parameters of 0.2 Å^{-1} and 0.25, respectively, were used.

3. Results and discussion

3.1 Structural properties

SnS crystallizes into several phases and polymorphs. Phase transition between these structural arrangements can take place relatively easy because of the variable valency. Basic polymorphs have structures with Cmcm, C2mb, Fm-3m, Pnma space groups [20].Whereas, the orthorhombic phase of SnS with Pnma space group is found as one which exists in normal conditions [20] [21].

To reveal the most energetically favored polymorph, we performed structural optimization for each modification. The studied polymorphs are schematically presented in Fig. 2.
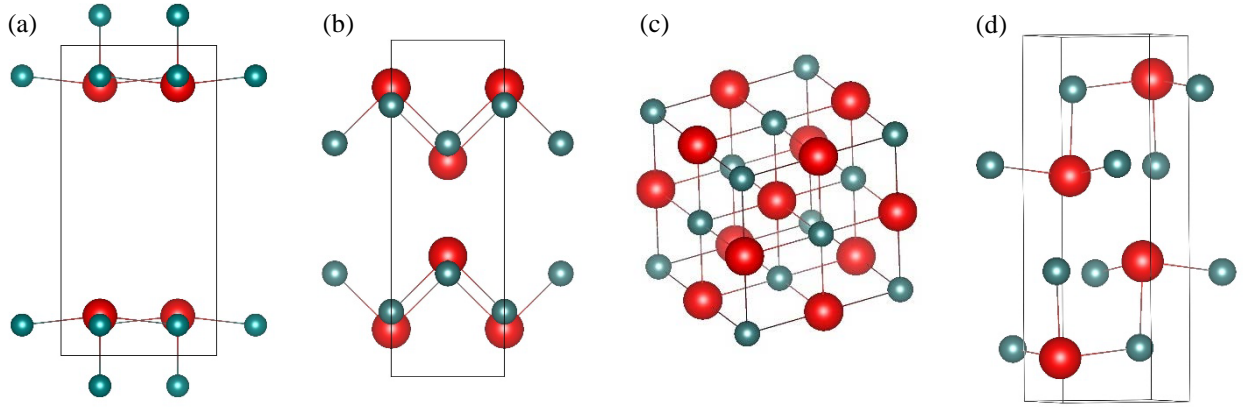
Fig.2 Polymorphs of SnS with different space group, where

(a) C2mb, (b) Cmcm, (c) Fm-3m, and (d) Pnma

The calculated total energy, equilibrium lattice parameters and volume for each of the considered polymorph are summarized in Table I and II. According to the Table I, polymorph Cmcm has the highest energy per pair of atoms -6.42 eV, while polymorph with Pnma space group has the lowest energy per pair of atoms -10.06 eV, meaning that Pnma is the most energetically favored structural modification. These results are consistent with those of Refs. [22] and [8]. Based on this result, all further calculations were performed using this polymorphic modification with Pnma space group.

Table I. – Calculated total energy for the polymorphs of SnS.

Energy per atom, eV	C2mb	Cmcm	F43m	Pnma
E_{Sn-S}	-9.74	-6.42	-9.80	-10.06

Values of total energy, and relaxed equilibrium lattice parameters of Pnma polymorph calculated with LDA, PBE, and HSE06 functionals, in comparison to experimental data from [23] are collected in Table II.

Table II. – Calculated total energy, calculated and experimental lattice parameters, volume for the Pnma polymorph

		LDA	PBE	HSE06	Exp.[a]
E_{Sn-S}, eV		-10.39	-10.06	-12.40	-
Lattice parameters, Å	a	10.96	11.51	11.33	11.20
	b	3.95	4.04	4.04	3.90

	c	4.20	4.30	4.36	4.30
	V, Å^3	181.89	199.95	199.42	193.53

^{a}*Experimental data of Ref. [23]*

Well known, that LDA usually underestimates values of lattice parameters compare to the experimentally measured once, while PBE and HSE06 overestimates the lattice constants. Result in that LDA provides strong binding in opposite to PBE and HSE06, which provide soft binding. In our case, an analysis of the obtained data from Table II shows that calculated values strongly depend on the functional were used. At that, LDA underestimates the volume by 6 % compare to experimental data, while PBE and HSE06 overestimate the volume by 3 % meaning that calculated data consist with mentioned trends.

3.2 Electronic properties of SnS using LDA

This section is devoted to describe the results of bandstructure obtained with LDA functional. In Figure 3 one can see the bandstructure and Density of States (DOS) of bulk SnS. The valence band maximum (VBM) is located near Z point, while the minimum of conduction band (CBM) is near Γ point. Obtained bandstructure corresponds to indirect bandgap. It is in an agreement with earlier reported theoretical data [6, 9] as well as some experimentally measured results [24]. However, it should be noted that there are some experimental works showing a direct bandgap in SnS, such as, for instance, photospectroscopy measurements in [3, 25, 26]

As we can see from the partial density of states, the major contribution to the valence band comes from s and p electrons, while the major contribution to the conduction band can be ascribed to p electrons. [3]

The bandgap, obtained as the difference between CBM and VBM, gives the value of 0.45 eV, while the experimentally measured one varies within the interval of 1.1-1.4 eV [2]. The underestimation of the bandgap is equal to 59 %.
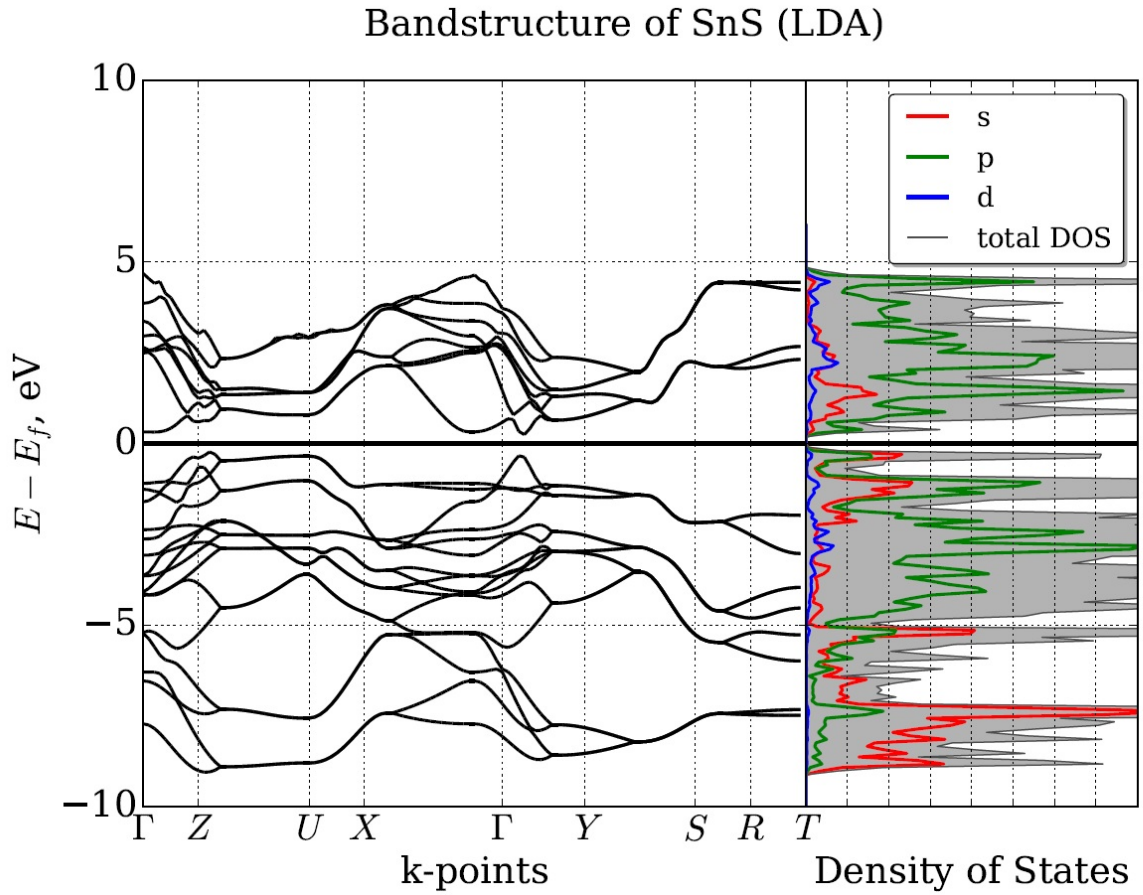
Fig. 3 The band structure and DOS SnS calculated by LDA functional

The comparison with the literature data shows that, the calculated in this work bandgap is in an agreement with another LDA study [7] giving the value of 0.4 eV, but do not match to some other works [10, 27]. Putting all the data together (see Table III) one can see that even if the same functional is used the bandgap value varies substantially.

Table III. –Bandgap, lattice parameters from recent LDA calculations

Eg, eV	Lattice const., Å	Volume, Å³	Equilibrium[a]/ Experimental[b]	Software	Reference
0.45	10.96 3.95 4.20	181.89	Relax.	VASP	This work
0.26	11.14 4.31, 3.96	190.21	Relax.	SIESTA	[27]
0.40	10.91, 3.88, 4.27	180.75	Relax.	Quantum Espresso	[7]
0.58	11.12, 3.95, 4.24	186.24	Relax.	GPAW	[10]
0.72	11.20, 3.99, 4.33	193.53	Exp.	Quantum Espresso	[7]

[a]*Equilibrium means that*

[b]*Experimental means that in calculations were used experimental lattice constants*

In fact, the values vary from 0.26 eV to 0.72 eV. Clearly, the calculated bandgaps using the same functional should not make any significant difference therebetween. We assume that a wide variation of bandgap is related to distinct lattice parameters, which were used in the calculations. Indeed, a calculation, which was performed using experimental lattice parameters shows a bigger bandgap than the results obtained using the same exchange-correlation functional but with equilibrium lattice parameters (see Table III). In order to check if our assumption correct or not, we have performed a calculation of bandgap with LDA functional using different lattice volumes of SnS cell from 181.9 to 199.8 Å³. The bandgap dependence on the volume of the unit cell is shown in Figure 4. The several calculated bandgap values from other works are marked on the graph using square dots. Our calculated bandgap using equilibrium LDA lattice parameters is marked by a triangle.
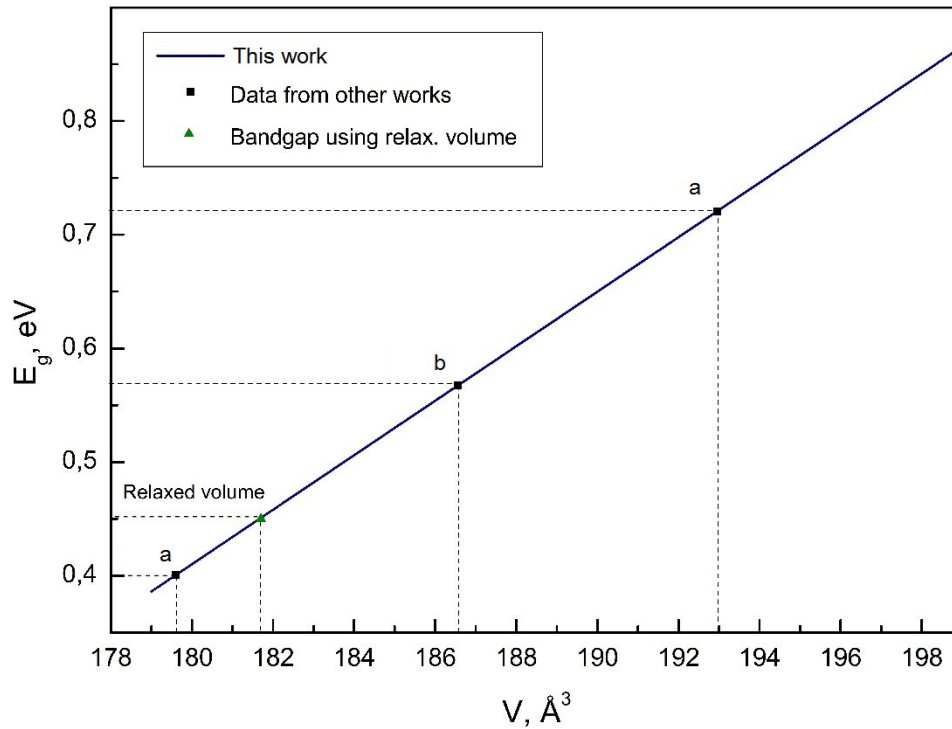
Fig.4 The calculated bandgap dependence on the volume of cell in comparison to [a] calculated data of Ref. [7] and [b] calculated data of Ref. [10]

As we can see from Fig.4, there is a linear dependence with a strong correlation between the value of bandgap and used volume of the unit cell. As the used volume increases, the calculated bandgap also increases. It is apparent that the previously published values of bandgap fit obtained straight line and concur within an error with our calculations. The reported values from [7] are equal to 0.4 and 0.72 eV, whereas our obtained results are 0.45 and 0.7 eV using the very similar lattice parameters. Furthermore, the value of bandgap from [10] is equal to 0.58 and close to our calculated result 0.6 eV, which is obtained using the same lattice parameters. The correlation between bandgap and lattice parameters of a material could be explained as an effect of tensile/compressive hydrostatic pressure, which appears under chosen conditions. The appearance of excessive pressure is related to using of not relaxed lattice parameters. The relaxed parameters are the equilibrium parameters, whereby structure has a normal pressure. Therefore, an excessive internal or external pressure appears from changing or insufficient relaxation of lattice parameters. This coincides with first principles calculations of bandgap dependence on the excessive pressure in SnS, which was reported at work [28]. The study shows decreasing of bandgap from 0.69 eV to 0 eV, with increasing of compressive pressure. Therefore, the wide variance of bandgap can be suggested to be explained by internal pressure which arises from insufficiently accurately chosen lattice parameters used in calculations.

3.3 Electronic properties of SnS using PBE

Electronic properties calculated based on PBE are slightly different compared to that of LDA calculations. The resulted bandstructure and DOS are shown in Fig. 5. As can be seen in Figure for PBE case, VBM is located near Z *k*-point, while CBM is near Y point as different to that LDA calculations. Nonetheless, PBE similar to LDA gives an indirect bandgap.

The partial density of states shows that the major contributors to the valence band comes from s and partly p electrons, while p electrons and partly s electrons are the major contributors to conduction band. The partial density of states has different features close to the edges of bandgap, which mostly corresponds to a shift of peaks compare to LDA case.
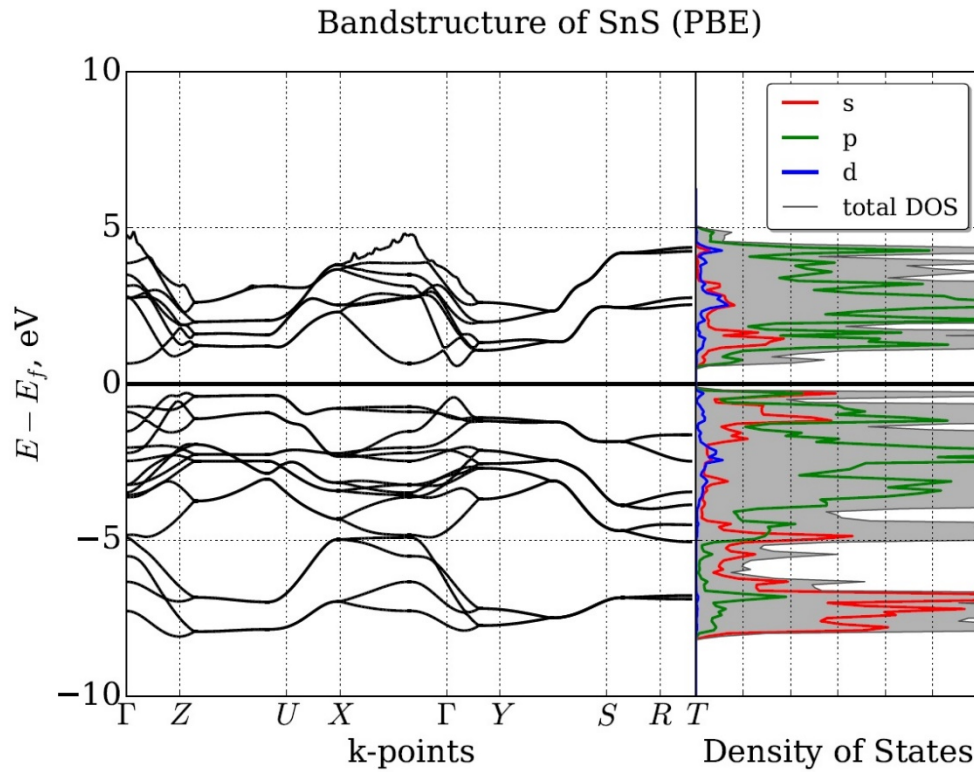

Fig. 5 The band structure and DOS of SnS calculated by PBE functional

Bandgap using PBE functional is larger than value from LDA by 0.15 eV but still underestimated and equal 0.6 eV, which is lower than experimental values 1.1-1.4 eV [2]. Table IV shows the bandgap, lattice parameters, which were obtained by PBE exchange-correlation functional from recent theoretical works as well as used software. The underestimation of the bandgap is equal to 45 %.

Table IV. – Bandgap, lattice parameters from recent PBE calculations

E_g, eV	Lattice const., Å	Volume, Å^3	Relaxed/ Experimental	Code	Reference
0.60	11.51, 4.04, 4.30	199.95	Relax.	VASP	This work
0.69	11.20, 3.99, 4.33	193.53	Exp.	ABINIT	[28]
0.75	11.55	-	-	VASP	[6]
0.90	11.42, 4.03, 4.41	202.83	Relax.	VASP	[9]
1.05	11.20, 3.99, 4.33	193.53	Exp.	WIEN2K	[11]

According to the data shown in Table IV, reported bandgap values change from paper to paper. The lowest calculated value using PBE was reported in [28] and equal to 0.69 eV, that is close to our calculated bandgap – 0.60 eV. The highest calculated bandgap is reported in [11] and equal to 1.05 eV. The same correlation as found in case of LDA between bandgap and lattice constants from the systematic analysis has not been detected. Therefore, we performed the calculation of bandgap based on PBE functional using different volume (Fig. 6). As one can see from Fig. 6, it is not clear that the calculated values of bandgap have a linear dependence on the used volume of unit cell compare to the same provided by LDA calculation because of the slight change of bandgap depending of the volume. However, there is a trend, which gives following results: the data from using an experimental unit cell volume (193.53 Å^3) shows the lowest value of bandgap equal to 0.50 eV, whereas increasing of unit cell volume up to 200.83 Å^3 gives the highest bandgap equal to 0.68 eV. The obtained trend suggests the same bandgap dependence on the volume of unit cell through the excessive tensile/ compressive hydrostatic pressures, as it was established in the previous section.
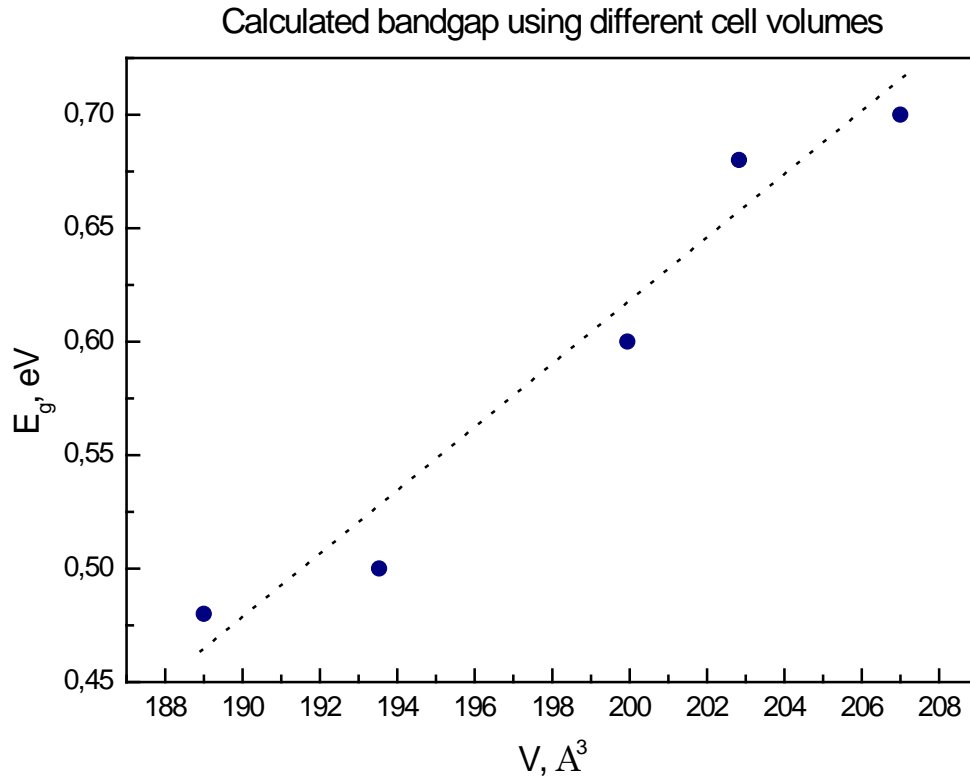
Fig. 6 The calculated based on PBE bandgap dependence on the volume of cell

3.4 Electronic properties of SnS using HSE06

The bandstructure from hybrid functional calculation (Fig. 7) shows that bandgap increased up to 1.1 eV without significant change in location of the band edges in reciprocal space compare to the LDA and PBE. It is in an agreement with reported values using hybrid functional [5] and experimental measurements 1.1-1.4 eV [2].
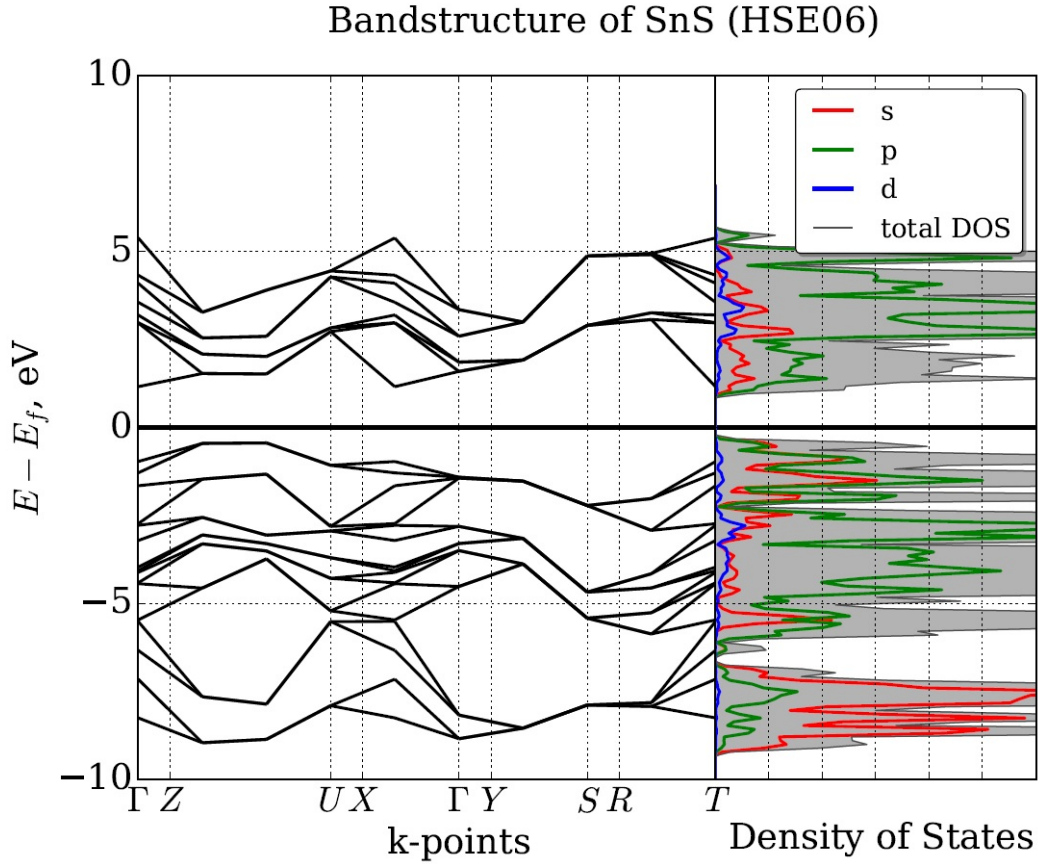
Bandstructure of SnS (HSE06)

Fig. 7 The band structure and DOS of SnS calculated by HSE06

We performed a full relaxation of lattice using HSE06 functional instead of using before-relaxed parameters from PBE. It should be noted, equilibrium constants obtained by HSE06 are significantly different from LDA and PBE calculations and using of relevant constants increases an accuracy of the calculation.

Our calculated bandgap value from HSE06 functional and reported once from other published data are collected in Table V. The obtained in this work bandgap is in an agreement with previously reported value, which is calculated by HSE06 [5]. As shown in Table V, the used lattice volume in our calculation is significantly larger than used one in the previous publication [5], but obtained bandgaps have a very small difference equal to 0.01 eV. Compared to mentioned above results, bandgap from HSE06 coincide with previously calculated one despite bandgap dependence on the volume of the used unit cell.

Table V. – Bandgap, lattice parameters from recent HSE06 calculations

	Eg, eV	Lattice const., Å	Volume	Relaxed/ Experimental	Code	Reference
HSE06	1.10	11.33, 4.04, 4.36	199.42	Relax.	VASP	This work
	1.11	11.20, 3.99, 4.33	193.53	Exp.	VASP	[5]

3.5 Comparison of the LDA, PBE, HSE06 functionals

In this section, we discuss a difference between obtained results from LDA, PBE, HSE06 functionals. As we discussed in previous sections, calculated bandgaps vary from 0.45 eV to 1.10 eV (Table V) depending on the used exchange-correlation functional. The obtained results are predictable according to well known fact – LDA underestimates bandgap on about of 60 percent, PBE underestimates bandgap on about 40 percent and HSE06 gives the best fit to experimental data.

Table V. – Summary of obtained bandgaps using different methods

Functional	E_g, eV	Experimental E_g, eV
LDA	0.40	
PBE	0.60	1.1-1.4[a]
HSE06	1.10	

[a]*Data of Ref.[2]*

To take a step closer to understanding the problem, let's consider next a short overview of the limitations of each method. LDA and PBE functionals are related to semi-local functionals, where the exchange correlation energy is given by a function depending on the electron density and derivative of electron density at each point of space. It is assumed that, the main contribution to the occurring errors in the semi-local functionals is given by the self-interaction. Self-interaction appears cause of the discontinuities, which are related to energy dependence on the electron density [29]. Whereas, the hybrid functional HSE06 is given by mixing of exact part of Hartree-Fock energy and PBE for a certain range. This approach allows partly removing the self-interaction and including a nondynamic correlation that improves a calculated bandgap up to the experimentally obtained value. The basic difference between functionals also could be seen from how they describe electronic structure besides bandgap. The

following part of the section is dedicated to consideration of deep levels in density of states depending on used exchange-correlation functional

Considering of deep levels in electronic structure shows that the bandstructures from each of functional have different features. PDOS within an interval of energy -9 to -4 eV is shown in Fig.8. The location and intensity of deep levels in obtained by LDA partial density of states is different compare to PBE and very similar compare to HSE06 functionals. Comparison of DOS spectra obtained from LDA and HSE06 functionals show that the location of peaks coincide with each other as well that major contributors within energy interval from -9 to -6 eV are s electrons in both. However, the peak shape and location is becoming different within the interval from -6 to -5 eV, while the major contributors are p and s electrons in both. In the case of PBE, DOS spectrum has an significant upward shift compared to LDA and HSE06. PBE functional provides that the major contributors within the interval from -9 to -5 eV are s electrons, though the contributors within the interval from -5 to -4 eV are p electrons.
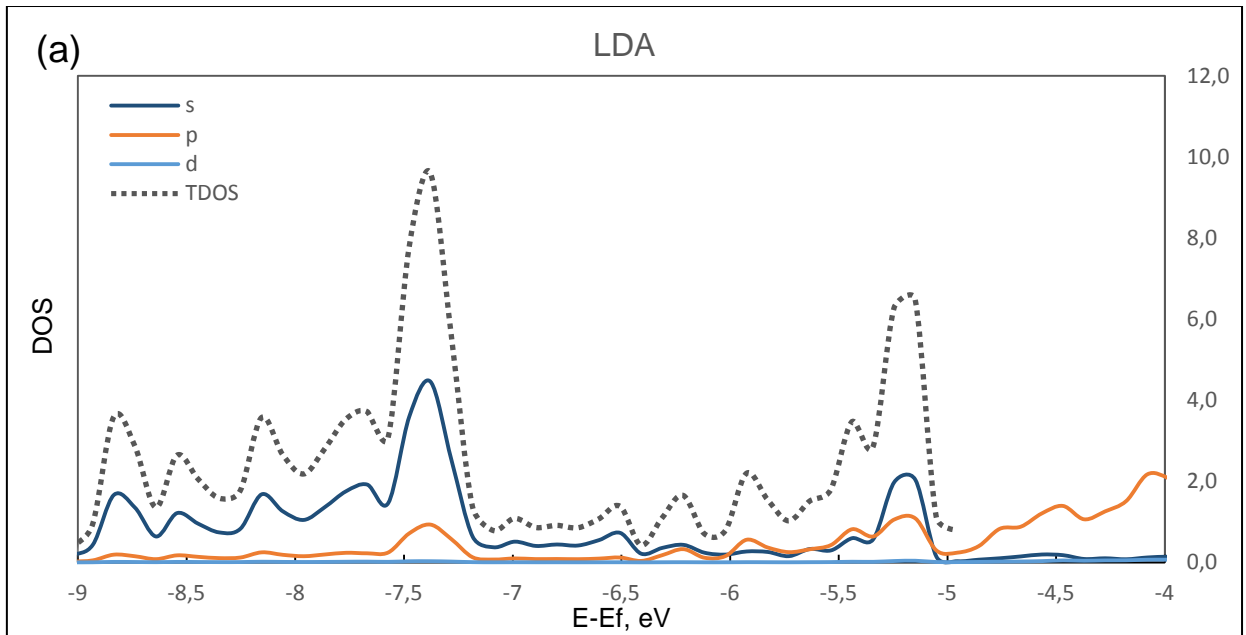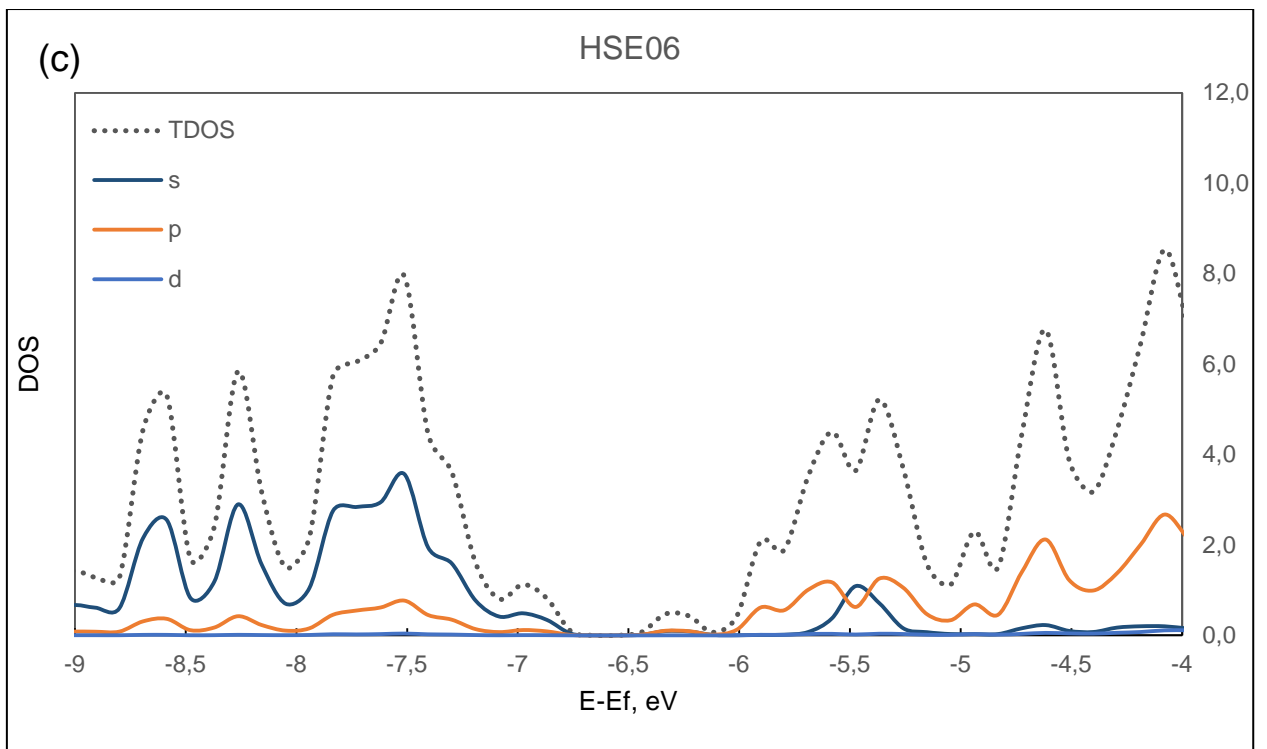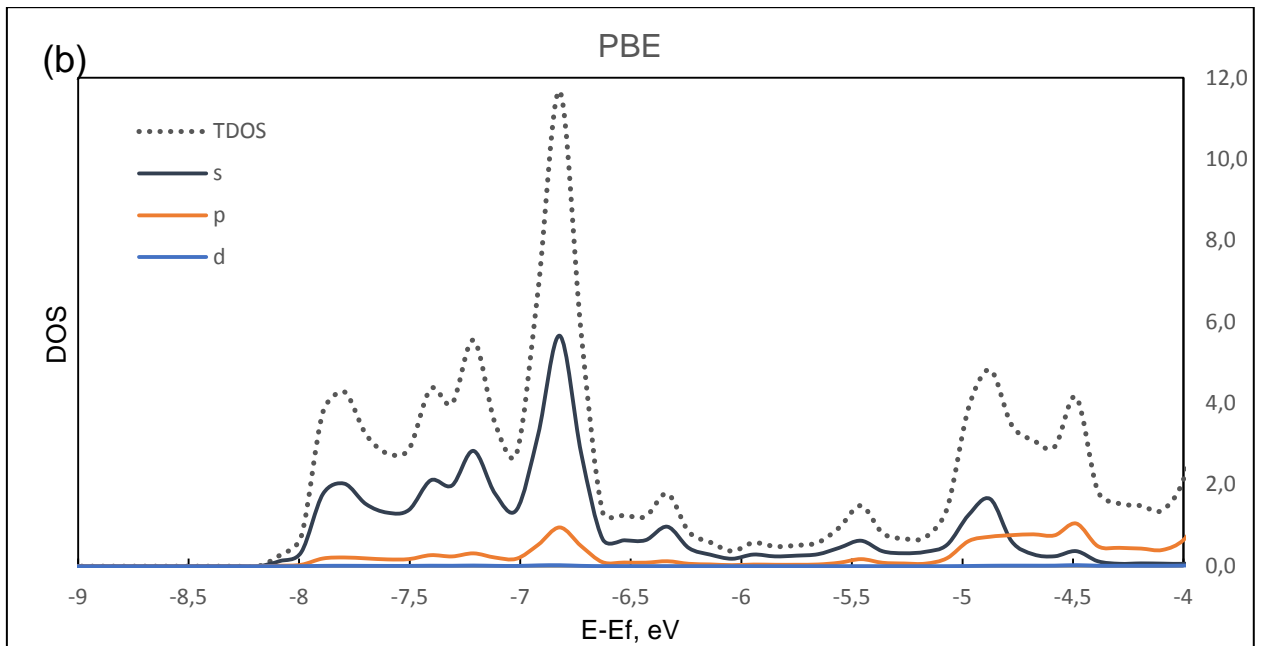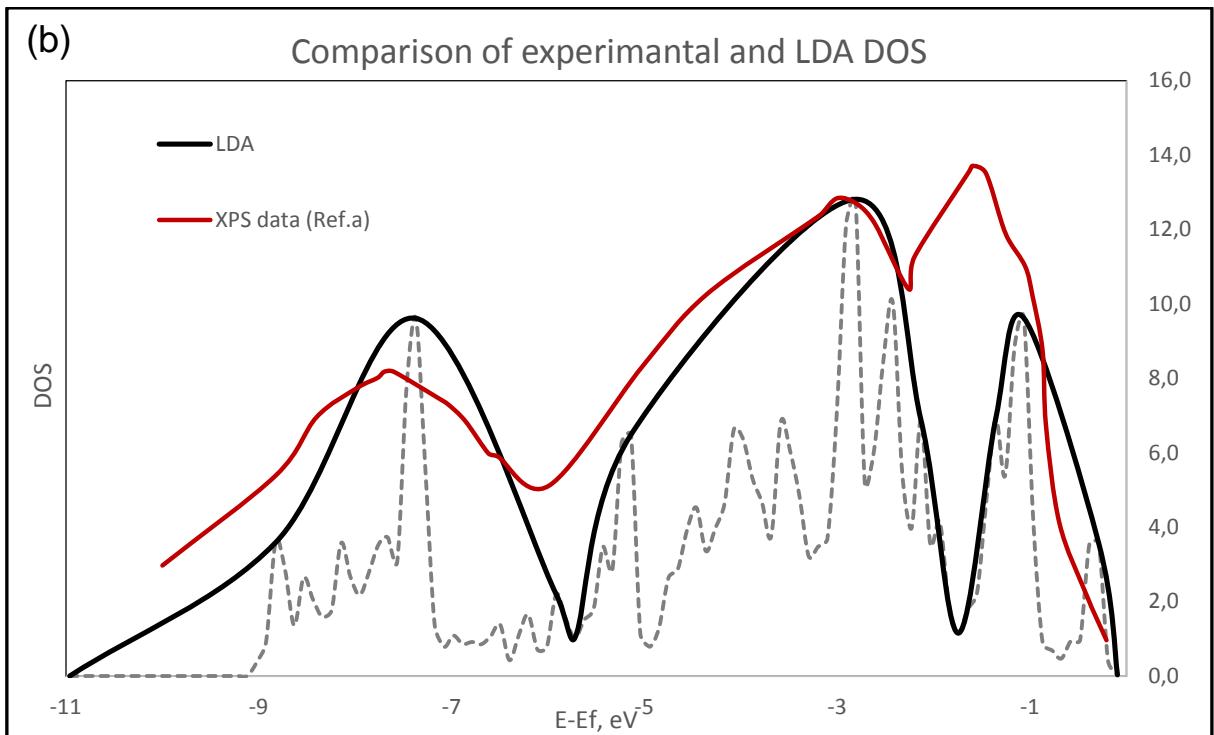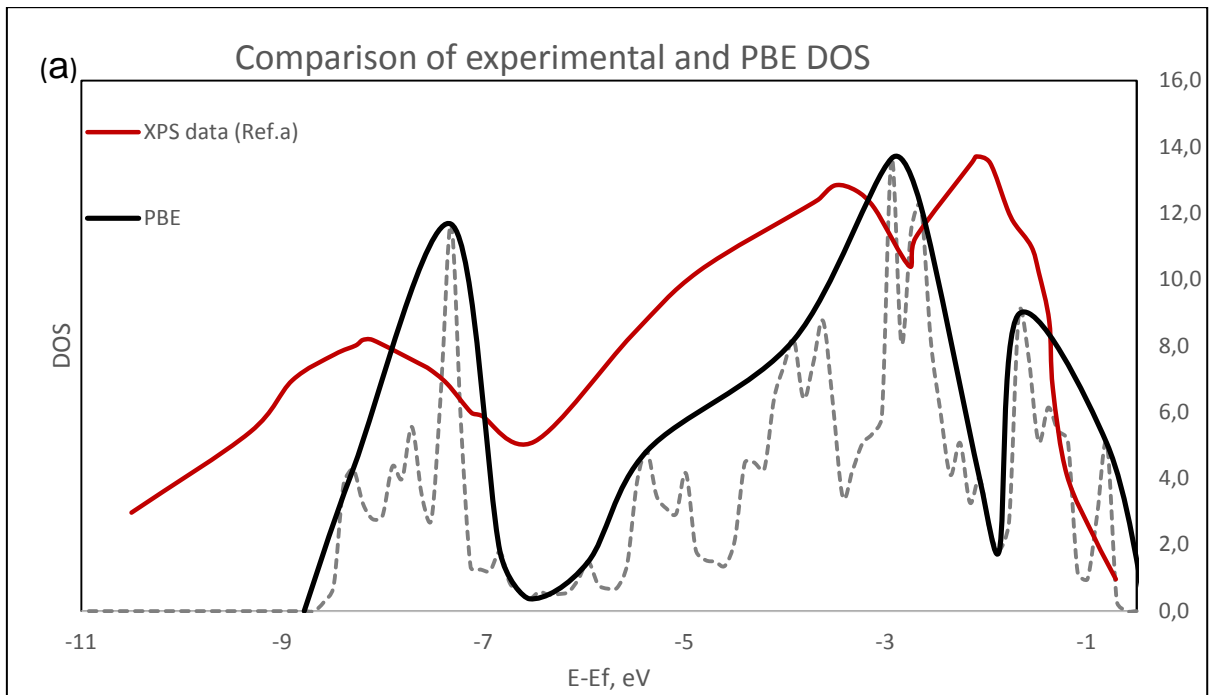
Fig. 8 Tin sulfide's theoretical partial density of states obtained from LDA– (a), PBE – (b) and HSE06 – (c)

If to compare the calculated DOS spectra of SnS with experimental data in order to consider the best match, then one can see in Fig. 9 the convolved DOS curves of the tin sulfide, together with experimentally measured valence band spectra, obtained from XPS measurements [30].

DOS from PBE calculations less coincide with XPS data, than DOS from LDA and HSE06. As we can see from Fig.9 (a) DOS from PBE has a shift compared to XPS data. Consequently, the location of peaks from PBE is a mismatch to the XPS data.
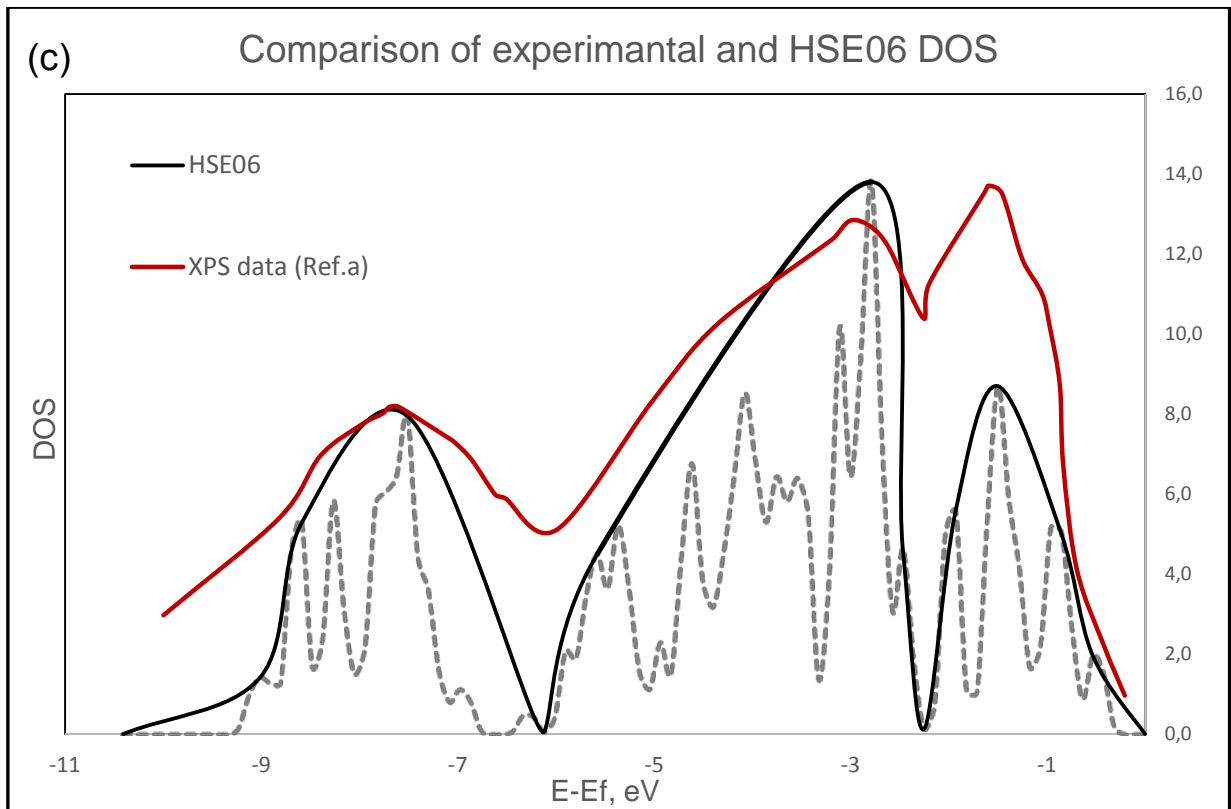
(a) Comparison of experimental and PBE DOS

(b) Comparison of experimantal and LDA DOS

(c)

Comparison of experimantal and HSE06 DOS

— HSE06

— XPS data (Ref.a)

DOS

E-Ef, eV

Fig. 9 – Calculated by PBE (a), LDA (b), HSE06 (c) and measured valence-band spectra of SnS

a Data of Ref. [30]

Despite the underestimation of bandgap, convolved LDA spectra Fig.9 (b) shows sufficient conjunction with experimental XPS of the valence band. There is a small shifting of the peak near to VBM. Whereas, spectra from HSE06 shows an agreement with XPS along all energies. The slight discrepancy of intensity appears in both. The comparison shows that DOS from PBE functional less fits experimental data, while LDA functional describes valence band better and gives spectra almost similar to that from HSE06.

Conclusions

In summary, we have studied different polymorphic modifications of tin sulfide with Cmcm, C2mb, Fm-3m, Pnma space groups, by first-principles calculations. Based on this study we have found that polymorph Pnma has the lowest energy compared to the other considered. We have calculated electronic properties such as bandstructure and density of states by several approaches (LDA, PBE, HSE06). Estimated bandgaps of SnS are 0.45 eV, 0.60 eV, and 1.10 eV respectively. The systematic analysis shows that the bandgap variation within one exchange-correlation functional is resulted from the appearance of a tensile/compressive hydrostatic pressure through using the nonequilibrium lattice parameters for calculation. The study of three functional applicability shows that the best reasonable functional, which sufficiently describes

bandstructure and DOS as well as bandgap is HSE06 exchange-correlation functional. However, even though less energy-consuming LDA underestimates the bandgap, the DOS spectrum from LDA functional is in agreement with experimentally measured XPS spectrum, which is similar to that of HSE06 and much better than General Gradient Approximation, PBE.

References

[1] R.J. Vera Steinmann , Katy Hartman , Rupak Chakraborty , Riley E. Brandt ,, Y.S.L. Jeremy R. Poindexter , Leizhi Sun , Alexander Polizzotti , Helen Hejin Park, a.T.B. Roy G. Gordon 3.88% Effi cient Tin Sulfi de Solar Cells using Congruent Thermal Evaporation, Adv. Mater., (2014).

[2] M.C.-P. Jacob A. Andrade-Arvizu, Osvaldo Vigil-Galan, SnS-based thin film solar cells: perspectives over the last 25 years, Journal of materials science materials in electronics, (2015).

[3] N.K.R. K.T. Ramakrishna Reddy, R.W. Miles, Photovoltaic properties of SnS based solar cells, Solar Energy Materials & Solar Cells, 90 (2006) 3041–3046.

[4] H.-J.S. A. Schneikart, A. Klein and W. Jaegermann, Efficiency limitations of thermally evaporated thin-film SnS solar cells, Journal Of Physics D: Applied Physics, 46 (2013) 7.

[5] R. Banai, L. Burton, S. Choi, F. Hofherr, T. Sorgenfrei, A. Walsh, B. To, A. Cröll, J. Brownson, Ellipsometric characterization and density-functional theory analysis of anisotropic optical properties of single-crystal α-SnS, Journal of Applied Physics, 116 (2014) 013511.

[6] J. Vidal, S. Lany, M. d'Avezac, A. Zunger, A. Zakutayev, J. Francis, J. Tate, Band-structure, optical properties, and defect physics of the photovoltaic semiconductor SnS, Applied Physics Letters, 100 (2012) 032104.

[7] E.K. Brad D. Malone, Quasiparticle band structures and interface physics of SnS and GeS, PHYSICAL REVIEW B, 87 (2013).

[8] L.A. Burton, Phase Stability and Composition of Tin Sulfide for Thin-Film Solar Cells, in: U.o. Bath, C.f.S.C. Technologies (Eds.), 2014.

[9] A.V.K. V. L. Shaposhnikov, V. E. Borisenko, J.-L. Lazzari, Structure, electronic and optical properties of tin sulfide, ScienceJet, 1 (2012).

[10] B.D.M. Georgios A. Tritsaris, and Efthimios Kaxiras, Structural stability and electronic properties of low-index surfaces of SnS, Journal of Applied Physics, 115 (2014).

[11] E.A.A. L. Makinistian, On the band gap location and core spectra of orthorhombic IV–VI compounds SnS and SnSe, Phys. Status Solidi B, 1 (2009) 183-191.

[12] J.P.P.a.A. Zunger, Self-interaction correction to density-functional approximations for many-electron systems, Phys. Rev. B 23 (1981) 5048.

[13] J.P. Perdew, K. Burke, M. Ernzerhof, Generalized Gradient Approximation Made Simple, Physical Review Letters, 77 (1996) 3865-3868.

[14] M.E. John P. Perdew, Kieron Burke, Rationale for mixing exact exchange with density functional approximations, J. Chem. Phys., 105 (1996).

[15] G.K. M. Shishkin, Self-consistent GW calculations for semiconductors and insulators, Phys. Rev. B, 75 (2007) 235102

[16] G. Kresse, J. Furthmüller, Efficient iterative schemes for \textit{ab initio} total-energy calculations using a plane-wave basis set, Physical Review B, 54 (1996) 11169-11186.

[17] P.E. Blöchl, Projector augmented-wave method, Physical Review B, 50 (1994) 17953-17979.

[18] B.G. Christoph Freysoldt, Tilmann Hickel, Jörg Neugebauer, Georg Kresse, Anderson Janotti, Chris G. Van de Walle, First-principles calculations for point defects in solids, REVIEWS OF MODERN PHYSICS, 86 (2014).

[19] J.S. Heyd, Gustavo E. Ernzerhof, Matthias, Hybrid functionals based on a screened Coulomb potential, The Journal of Chemical Physics, 118 (2003) 8207-8215.

[20] R.C.S.a.Y.A. Chang, The S-Sn (Sulfur-Tin) System Bulletin of Alloy Phase Diagrams, 7 (1986) 269-273.

[21] L.A.B.a.A. Walsh, Phase Stability of the Earth-Abundant Tin Sulfides SnS, SnS_2, and Sn_2S_3, The Journal of Physical Chemistry C, 116 (2012) 24262−24267.

[22] V.S. R. Chakraborty, N. M. Mangan, R. E. Brandt, J. R. Poindexter, R. Jaramillo, J. P. Mailoa, K., A.P. Hartman, C. Yang, R. G. Gordon, T. Buonassisi, Non-monotonic effect of growth temperature on carrier collection in SnS solar cells, Applied Physics Letters, 106 (2015).

[23] J.P. T. CHATTOPADHYAY, H. G. VON SCHNERING, NEUTRON DIFFRACTION STUDY OF THE STRUCTURAL PHASE TRANSITION IN SnS AND SnSe, Phys. Chem. Solids 47 (1986) 879-885.

[24] C.H. W. Albers, H. J. Vink, J. D. Wasscher, Investigations on SnS, Journal of Applied Physics, 32 (1961).

[25] in, pp. Spectrofotometr.

[26] Y.M. M. Sugiyama, T. Shimizu, K. Ramya, C. Venkataiah, T. Sato,, K.T.R. Reddy, Journal of Applied Physics, 50 (2011).

[27] S.S. Husnu Koc, Selami Palaz, Oral Oltulu, Amirullah M. Mamedov, Ekmel Ozbay, Mechanical, electronic, and optical properties of the A4B6 layered ferroelectrics: Ab initio calculation, Phys. Status Solidi C, 12 (2015).

[28] E.A.A. L. Makinistian, Study of the hydrostatic pressure on orthorhombic IV–VI compounds including many-body effects, Computational Materials Science, 50 (2011) 2872–2879.

[29] J.P. PERDEW, Density Functional Theory and the Band Gap Problem, International Journal of Quantum Chemistry Quantum Chemistry Symposium, 19 (1986) 497-523.

[30] L.A.B. Thomas J. Whittles, Jonathan M. Skelton, Aron Walsh, T. D. Veal, and Vin R Dhanak, Band Alignments, Valence Bands and Core Levels in the Tin Sulfides SnS, SnS2 and Sn2S3: Experiment and Theory, Chemistry of Materials, (2016).